Self-Induced Polar Order of Active Brownian Particles in a Harmonic Trap

Marc Hennes, Katrin Wolff, and Holger Stark
Institut für Theoretische Physik, Technische Universität Berlin, Hardenbergstraße 36, 10623 Berlin, Germany
(Received 6 February 2014; published 13 June 2014)

Hydrodynamically interacting active particles in an external harmonic potential form a self-assembled fluid pump at large enough Péclet numbers. Here, we give a quantitative criterion for the formation of the pump and show that particle orientations align in the self-induced flow field in surprising analogy to ferromagnetic order where the active Péclet number plays the role of inverse temperature. The particle orientations follow a Boltzmann distribution $\Phi(\mathbf{p}) \sim \exp(Ap_z)$ where the ordering mean field A scales with the active Péclet number and polar order parameter. The mean flow field in which the particles' swimming directions align corresponds to a regularized Stokeslet with strength proportional to swimming speed. Analytic mean-field results are compared with results from Brownian dynamics simulations with hydrodynamic interactions included and are found to capture the self-induced alignment very well.

DOI: 10.1103/PhysRevLett.112.238104 PACS numbers: 87.10.Mn, 47.57.J−, 83.10.Mj, 87.18.Gh

Introduction.—Understanding the nonequilibrium behavior of self-propelled particles is one of the major challenges at the interface of physics, biology, and also chemical engineering [1,2]. Interacting active particles may show exotic phenomena such as swirling motion [3], or exhibit dynamic clustering [4,5] and motility-induced phase separation [6–10]. Their collective motion drives macroscopic fluid flow as in bioconvection [11] or vortex formation [12]. Hydrodynamic interactions between microswimmers crucially determine their collective patterns [13–20], while external fluid flow leads to aggregation [21], trapping [22], and nonlinear swimming dynamics [23].

In order to understand the collective dynamics of active particles and their steady-state distributions, they are often mapped onto passive systems that move in effective potentials [24–26]. However, for interacting particles there is no general route for identifying an equilibrium counterpart [1,6,10].

The system we investigate here is composed of self-propelled or active Brownian particles whose swimming directions undergo rotational diffusion in a harmonic trap. Bacteria or both active and passive colloids confined in optical traps have attracted experimental [27–29] as well as theoretical [24,30–33] interest. Passive colloids are operated in nonequilibrium by switching the trapping force [31], while active particles are intrinsically out of equilibrium [24,32,33]. Run-and-tumble particles in lattice Boltzmann simulations develop a pump state which breaks the rotational symmetry of the harmonic trap and cause a macroscopic fluid flow [32]. Here, we demonstrate similar behavior for active Brownian particles which interact by hydrodynamic flow fields. However, more importantly, we explain the emerging orientational order of particles by mapping the self-induced alignment of swimmers in a harmonic potential onto an equilibrium system which exhibits ferromagnetic order.

To this end, we first establish an intuitive criterion for the formation of the pump and then introduce a mean-field description for the fully formed pump state. The mean-field system shows a striking analogy to the Weiss molecular field in ferromagnetism and reproduces our Brownian dynamic simulations.

The system also bears some similarity to the vortex formation in *Daphnia* populations [12] caused by irradiation with light, where the apparent attraction towards the center of the light spot has also been modeled by a harmonic potential [34]. The crucial difference, however, is that *Daphnia* swim towards the light by phototaxis whereas in the system discussed here the harmonic potential exerts a body force on the swimmers. One focus of this work is thus on the self-induced polar order of active particles and how it is mapped on a passive system with very different underlying physics.

The model.—We consider a dilute suspension of N self-propelled particles with constant propulsion speed v_0, whose leading hydrodynamic interactions are modeled by (far-field) mobility tensors $\boldsymbol{\mu}_{ij}$. Particles are spherical with an internal orientation vector $\mathbf{p}_i$, as realized, for example, in active colloids [5,9], and they swim with velocity $v_0\mathbf{p}_i$. The Langevin equations of motion for the position $\mathbf{r}_i$ and orientation $\mathbf{p}_i$ of particle i then are $\dot{\mathbf{r}}_i = \mathbf{v}_i$, $\dot{\mathbf{p}}_i = \boldsymbol{\omega}_i \times \mathbf{p}_i$ with

$$\mathbf{v}_i = v_0\mathbf{p}_i + \sum_{j=1}^{N} \boldsymbol{\mu}_{ij}^{tt}\mathbf{F}_j + \sum_{j=1}^{2N} \mathbf{H}_{ij}\boldsymbol{\xi}_j + \sum_{j\neq i}^{N} \mathbf{u}_{\mathrm{SS},j}(\mathbf{r}_{ij}),$$

$$\boldsymbol{\omega}_i = \sum_{j=1}^{N} \boldsymbol{\mu}_{ij}^{rt}\mathbf{F}_j + \sum_{j=1}^{2N} \mathbf{H}_{(i+N)j}\boldsymbol{\xi}_j + \sum_{j\neq i}^{N} \boldsymbol{\omega}_{\mathrm{SS},j}(\mathbf{r}_{ij}).$$

The particle velocity $\mathbf{v}_i$ thus consists of the self-propulsion term $v_0\mathbf{p}_i$ along the particle's orientation vector, the

contribution from the harmonic trapping forces acting on all particles, $\mathbf{F}_j = -k_{\mathrm{trap}}\mathbf{r}_j$, a stresslet velocity term $\mathbf{u}_{\mathrm{SS}}$ caused by the active swimming of all other particles with $\mathbf{r}_{ij} = \mathbf{r}_i - \mathbf{r}_j$, and the thermal noise term $\sum_{j=1}^{2N} \mathbf{H}_{ij}\boldsymbol{\xi}_j$. Here, $\boldsymbol{\xi}_j$ is a three-component vector and contains time-uncorrelated Gaussian variables with zero mean and unit variance for translational or rotational noise. The noise components are coupled to each other by the 3×3 amplitude matrices $\mathbf{H}_{ij}$, which are determined by the fluctuation-dissipation theorem. Further details are found in the Supplemental Material [35]. The swimmers interact hydrodynamically via the second and fourth term in $\mathbf{v}_i$. We consider hydrodynamic interactions up to second order in $1/r$, with r the swimmer distance, and use for the translational mobility $\boldsymbol{\mu}_{ij}^{tt}$ the Oseen tensor. The velocity stresslet $\mathbf{u}_{\mathrm{SS},j}(\mathbf{r}) = \beta v_0 \frac{3a^2}{4r^2}[-3(\mathbf{p}_j \cdot \hat{\mathbf{r}})^2 + 1]\hat{\mathbf{r}}$, with $\hat{\mathbf{r}} = \mathbf{r}/r$ and particle radius a, determines whether a particle is an extensile (pusher, $\beta < 0$), contractile (puller, $\beta > 0$), or neutral ($\beta = 0$) swimmer. Unless stated otherwise, we set $\beta = 0$ and use the neutral swimmer as default. Additionally, excluded volume interactions between particles keep swimmers from approaching closer than their diameter $2a$ (see Supplemental Material [35]).

Angular velocity likewise consists of a deterministic part due to the vorticity caused by the trapping force, the vorticity due to the swimmers' flow dipoles $\boldsymbol{\omega}_{\mathrm{SS}} = (\nabla \times \mathbf{u}_{\mathrm{SS}})/2$, and thermal rotational noise $\mathbf{H}_{(i+N)j}\boldsymbol{\xi}_j$. The mobility tensor $\boldsymbol{\mu}_{ij}^{rt}$ couples translational to rotational motion and in leading order of $1/r^2$ is given in the Supplemental Material [35]. We simulate the collective dynamics of active particles using Brownian dynamics simulations with hydrodynamic interactions following an extended form of the algorithm by Ermak and McCammon [36], where the self-propulsion and swimming terms are included.

Pump formation.—In steady state, noninteracting active particles accumulate at or near the surface of a sphere where active swimming and trapping force cancel each other. The particles' horizon has the characteristic radius $r_{\mathrm{hor}} = a\mathrm{Pe}/\alpha$ [24], where a is the particle radius, $\mathrm{Pe} = v_0 a/D$ the active Péclet number, and $\alpha = k_{\mathrm{trap}}a^2/(k_B T)$ the trapping Péclet number with translational diffusion coefficient $D = k_B T/(6\pi\eta a)$. The spherical symmetry, however, is spontaneously broken when hydrodynamic interactions are included. At sufficiently large Pe, particles assemble into a pump in a more tightly packed region, where they align their swimming directions and produce a macroscopic fluid flow [32]. The situation is sketched in Fig. 1 (left) and accompanying videos can be found in the Supplemental Material [35].

Figure 1 (right) gives the state diagram for pump formation. A simple scaling argument predicts pump formation against thermal noise (lower solid line in the diagram) and can be derived from a comparison of diffusive and advective time scales for rotational motion. Suppose

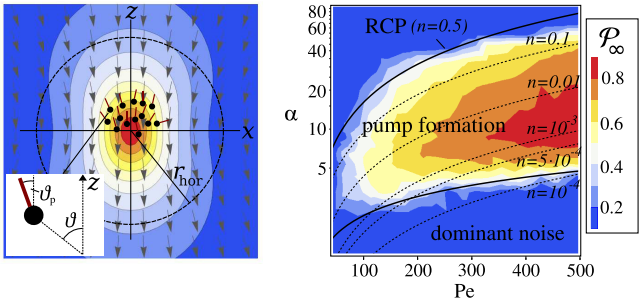

FIG. 1 (color online). Left: sketch of the fluid pump. Active particles concentrate in the upper half sphere and align their orientations along the vertical. The resulting flow field is illustrated by a regularized Stokeslet. The dashed black circle with radius r_{hor} is the particles' horizon. Right: state diagram of pump formation in active (Pe) versus trapping (α) Péclet numbers. The mean orientation of the particles, $\mathcal{P}_\infty$, is color coded. The lower solid curve, $\alpha \propto \sqrt{\mathrm{Pe}/N}$, separates the region of pump formation from the region of dominant rotational noise. Along the dashed lines density n is constant. At very high densities the active particles become randomly close packed (RCP) and cannot form a pump (upper solid curve).

we start with noninteracting active particles which for large Pe accumulate uniformly at or near the horizon sphere with radius r_{hor}. We now switch on the Stokeslets generated by the harmonic trapping forces. Since particles are stuck at the horizon sphere, the main effect from their neighbors comes from the flow field's vorticity ω_{HI}. It rotates a particle's swimming direction away from the radial direction. Particles move towards each other and generate denser particle regions. These become unstable along the radial direction due to the collective flow field and pump formation sets in. However, rotational diffusion acts against vorticity ω_{HI} and we expect pump formation to set in when the characteristic time scales for rotational diffusion and advection are similar, $1/D_R \sim 1/\omega_{\mathrm{HI}}$, where D_R is the rotational diffusion coefficient [37] . In the Supplemental Material [35] we estimate the vorticity disturbance as $\omega_{\mathrm{HI}} = k_{\mathrm{trap}} r_{\mathrm{hor}}/(8\pi\eta r_{\mathrm{nn}}^2)$ with the nearest-neighbor distance $r_{\mathrm{nn}} \approx 4r_{\mathrm{hor}}/\sqrt{N}$ and give further details of the calculations. Using definitions for D_R, r_{hor}, and α, the pump formation criterion $1/D_R \sim 1/\omega_{\mathrm{HI}}$ then becomes $\alpha \sim \sqrt{\mathrm{Pe}/N}$.

This rough estimate reproduces the scaling α versus Pe for the onset of pump formation quite well [see lower solid line in Fig. 1 (right) with an appropriately chosen proportionality factor]. To indicate the alignment of particle orientations in the steady state, we use the polar order parameter $\mathcal{P}_\infty = \lim_{t\to\infty} |\sum_{i=1}^{N} \mathbf{p}_i(t)|/N$ [17]. For very dense systems, particles become close packed and no pump is formed as the upper solid curve at constant density $n = 0.5$ in Fig. 1 (right) shows. At such high densities, however, the assumption of far-field interactions also no longer holds. In the following we concentrate on dilute systems and, unless stated otherwise, follow the path of the

dashed line with mean density $n = 10^{-3}$. To realize a constant density for different Pe, we fix the particle number $N = 100$ and keep the effective trap volume constant by varying the trapping Péclet number α alongside the active Péclet number Pe to ensure $r_{\mathrm{hor}} \propto \alpha/\mathrm{Pe} = \mathrm{const}$.

Mean-field theory for self-induced order.—In order to gain analytical insight, we reduce the Smoluchowski equation for the N-particle distribution function to a mean-field equation for the one-particle distribution $\psi(\mathbf{r}, \mathbf{p})$. The collective dynamics due to hydrodynamic interactions is taken into account by a mean flow field $\mathbf{u}(\mathbf{r})$ generated by all the particles. It is independent of time, once the pump has formed. The Smoluchowski equation governing the effective one-particle dynamics is

$$\partial_t \psi(\mathbf{r}, \mathbf{p}) = -\nabla \cdot \mathbf{J}_T - \mathcal{R} \cdot \mathbf{J}_R \quad \text{with} \quad \mathcal{R} = \mathbf{p} \times \nabla_{\mathbf{p}}. \tag{1}$$

We use the translational flux $\mathbf{J}_T = [v_0 \mathbf{p} + \mu_t \mathbf{F}_{\mathrm{ext}}(\mathbf{r}) + \mathbf{u}(\mathbf{r})]\psi(\mathbf{r}, \mathbf{p})$ and the rotational flux $\mathbf{J}_R = [(\nabla \times \mathbf{u}(\mathbf{r}))/2 - D_R \mathcal{R}]\psi(\mathbf{r}, \mathbf{p})$. Translational diffusion is neglected in $\mathbf{J}_T$ because of Péclet numbers $\mathrm{Pe} \gtrsim 100$, whereas rotational diffusion still needs to be included. As we assume the flow field $\mathbf{u}$ to be independent of time, Eq. (1) only describes the dynamics close to a fully formed pump state and we will just attempt to determine the steady state distribution $\psi(\mathbf{r}, \mathbf{p})$.

Strictly speaking, the collective flow field follows self-consistently from the distribution $\psi(\mathbf{r}, \mathbf{p})$ by integrating over all particle contributions, $\mathbf{u}(\mathbf{r}) = \int \boldsymbol{\mu}(\mathbf{r} - \mathbf{r}') \mathbf{F}_{\mathrm{ext}}(\mathbf{r}') \psi(\mathbf{r}', \mathbf{p}') d\mathbf{r}' d\mathbf{p}'$. Here, however, we first determine the flow field from the full N-particle simulations, argue that it is well represented by a regularized Stokeslet, and only check *a posteriori* that our resulting mean-field density gives rise to the same flow field.

To quantify the flow field $\mathbf{u}(\mathbf{r})$, Fig. 2 shows the directional average for the absolute value of its Fourier transform $\tilde{\mathbf{u}}(\mathbf{k})$. The average goes over all directions of wave vector $\mathbf{k}$ keeping wave number k fixed. Before taking the Fourier transform, the flow field has been averaged over 100 uncorrelated simulation snapshots in the steady state to suppress fluctuations. We find that in the parameter range, where the pump is fully formed, the strength of the flow field $\mathbf{u}$ is simply proportional to the particle swimming speed v_0. As Fig. 2 demonstrates, for active Péclet number $\mathrm{Pe} = 100$ the pump has not yet fully formed but for $\mathrm{Pe} = 200$ to 500 all data fall on a single master curve when rescaled by v_0. They agree very well with the flow field of a regularized Stokeslet [38],

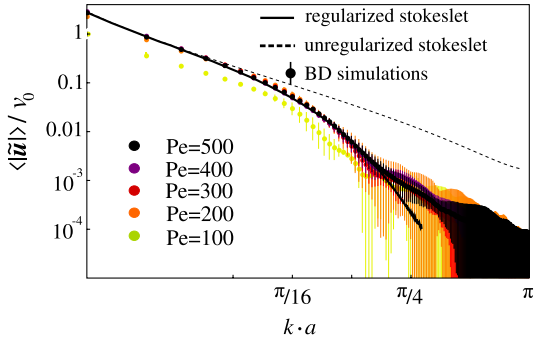

FIG. 2 (color online). Directional average for the absolute value of the Fourier transform of fluid velocity, $\langle|\tilde{\mathbf{u}}(\mathbf{k})|\rangle$, plotted versus wave number k. Results obtained from the Brownian dynamics (BD) simulations (colored dots) are compared with a regularized Stokeslet (solid line coinciding with data points) and a Stokeslet without regularization (dashed line).

$$\mathbf{u}_{\mathrm{reg}}(\mathbf{r}) = -\frac{v_0 \epsilon}{2(r^2 + \epsilon^2)^{3/2}} [\mathbf{1}(r^2 + 2\epsilon^2) + \mathbf{r} \otimes \mathbf{r}] \mathbf{e}_z, \tag{2}$$

also for the regions *inside* the pump (see Fig. 2, solid line). Here, the flow field deviates from an unregularized Stokeslet (dashed line) and only in the far field (small k) does the flow field become a conventional Stokeslet. The regularization parameter ϵ is used as a fit parameter but it turns out that it coincides with the radius of the region populated by active particles and thus can be interpreted as the pump radius. For large wave numbers k, the simulated flow field starts to differ from $\mathbf{u}_{\mathrm{reg}}$ as fluctuations on the scale of several particle radii become visible.

We now make an ansatz for the particle distribution $\psi(\mathbf{r}, \mathbf{p})$ and assume that particle orientations always point radially outward, $\psi(\mathbf{r}, \mathbf{p}) = \Phi(\mathbf{p}) f(r) \delta(\cos(\theta) - \cos(\theta_p)) \delta(\varphi - \varphi_p)$. Here, θ and φ are the spherical coordinate angles of position and θ_p and φ_p those of orientation. The polar angles θ and θ_p are both measured against the main axis of the pump [see also the sketch in Fig. 1 (left)]. The assumption of parallel orientation and position vector is motivated by the system without hydrodynamic interactions at high Péclet numbers. Here, particles quickly swim to the horizon where the trapping force cancels their self-propulsion. With interactions included, the assumption of parallel orientation and position vector still holds approximately (see Supplemental Material [35]). Integrating Eq. (1) over particle position using the ansatz for $\psi(\mathbf{r}, \mathbf{p})$, we arrive at the equation for the orientational distribution function,

$$\partial_t \Phi(\mathbf{p}) = -\mathcal{R} \cdot [\langle \boldsymbol{\omega} \rangle(\mathbf{p}) - D_R \mathcal{R}] \Phi(\mathbf{p}), \tag{3}$$

where the mean vorticity of the collective flow field is determined for the regularized Stokeslet of Eq. (2): $\langle \boldsymbol{\omega} \rangle(\mathbf{p}) = -D_R A \sin(\theta_p) \mathbf{e}_{\varphi_p}$ with $A = \mathrm{Pe} \int_0^\infty (\epsilon a (5\epsilon^2 + 2r^2)/3(\epsilon^2 + r^2)^{5/2}) r^3 f(r) dr$. Equation (3) can then be solved in steady state and the orientational distribution function becomes $\Phi(\mathbf{p}) = e^{A \cos(\theta_p)}/\mathcal{N}$, where $\mathcal{N}$ is a normalization factor. Figure 3 (top) shows $\Phi(\mathbf{p})$ for different active Péclet numbers in very good agreement with Brownian dynamics simulations. The parameter ϵ and the radial distribution $f(r)$ necessary to determine the constant A for the analytic result have been extracted from the fits of the flow field and the simulations, respectively.

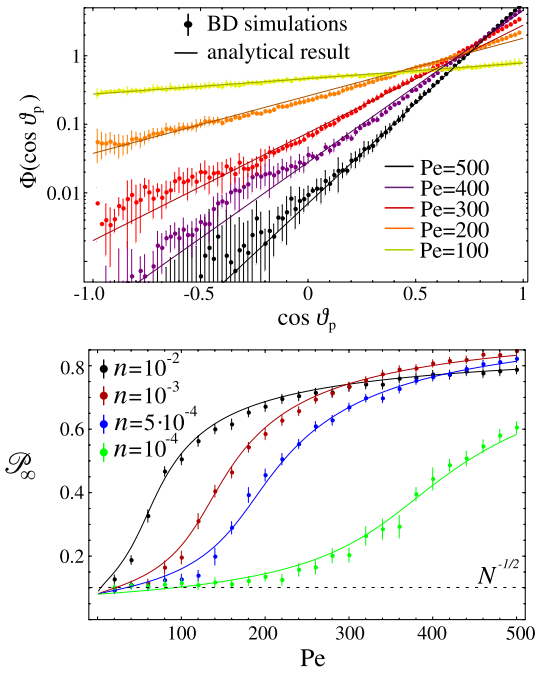

FIG. 3 (color online). Top: orientational distribution functions for different values of particle activity Pe at fixed average density $n = 10^{-3}$. The simulation results (dots) are very well reproduced by $\Phi(\cos\theta_p) \sim \exp(A\cos\theta_p)$ (solid lines), where A can be derived analytically. Bottom: particle alignment $\mathcal{P}_\infty$ for increasing activity Pe at different densities. The simulation results (dots) again agree very well with the analytic result $(\mathcal{P}_\infty - N^{-1/2})/\mathcal{P}_\infty^{\max} = \mathcal{L}(3(\mathrm{Pe}\mathcal{P}_\infty/\mathrm{Pe}_c)^\gamma)$ (solid lines).

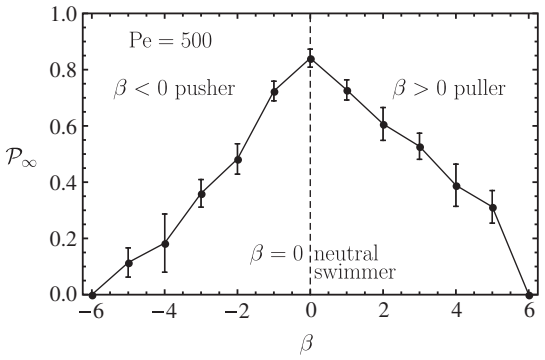

FIG. 4. Influence of swimmer dipole fields on the pump formation at activity Pe = 500 and volume fraction $n = 10^{-3}$. Mean polar order $\mathcal{P}_\infty$ plotted versus swimmer type β.

All particles thus create a mean flow field in which single swimmers align, in analogy to Weiss theory for ferromagnetism using a molecular field. Here the regularized Stokeslet or, more precisely, the field strength A takes the role of the molecular magnetic field and mean polar order $\mathcal{P}_\infty$ that of magnetization. This analogy can be made more explicit by looking at the overall alignment $\mathcal{P}_\infty = \int_0^{2\pi}\int_{-1}^{1} \mathbf{p}\Phi(\mathbf{p})d\varphi_p d\cos(\theta_p)$, which evaluates to $\mathcal{P}_\infty = \mathcal{L}(A) = \coth(A) - 1/A$ with the Langevin function $\mathcal{L}(A)$ as encountered in the classical theory of magnetism [39]. Importantly, the field strength A depends in turn on the alignment $\mathcal{P}_\infty$ and we find in our simulations $A \propto (\mathrm{Pe}\mathcal{P}_\infty)^\gamma$ with an exponent γ close to 1 for low densities and decreasing for higher densities (see Supplemental Material [35]). So, we indeed have a formal analogy to the Weiss molecular field generalized to an exponent $\gamma \leq 1$. The active Péclet number Pe takes the role of inverse temperature and a critical Pe can be determined.

Figure 3 (bottom) shows alignment curves for various values of density n. Because of the finite number of particles N, the curves are shifted from 0 to $\mathcal{P}_\infty = N^{-1/2}$ for no alignment. Similarly, total alignment $\mathcal{P}_\infty = 1$ cannot be attained because the shape of the pump and the excluded volume of the particles prohibit completely parallel particle orientations. The latter is taken into account via a geometric parameter $\mathcal{P}_\infty^{\max}$. The implicit equation for $\mathcal{P}_\infty$ becomes $(\mathcal{P}_\infty - N^{-1/2})/\mathcal{P}_\infty^{\max} = \mathcal{L}(3(\mathrm{Pe}\mathcal{P}_\infty/\mathrm{Pe}_c)^\gamma)$, which fits the data very well when numerically solved for $\mathcal{P}_\infty$ with the critical Péclet number Pe_c and the geometric parameter $\mathcal{P}_\infty^{\max}$ as fitting parameters. The exponent $\gamma = 1.0$ for $= 10^{-4}$ but decreases for higher densities and is only $\gamma = 0.5$ for $n = 10^{-2}$, which is likely due to excluded volume effects.

We also investigated the effect of the velocity dipoles ($\beta \neq 0$ [40]) due to the particles' swimming and found flow stresslets to hinder alignment (Fig. 4). This is in agreement with previous studies on suspensions of active particles [17,19]. Neutral swimmers ($\beta = 0$) show the strongest ordering meaning that the alignment of swimmers is mediated solely by the Stokeslets due to the trapping force, as assumed in our calculations. For biologically relevant parameters $\beta \in [-1, 1]$ (see Ref. [17]) the reduction in the mean polar order $\mathcal{P}_\infty$ is small and the mean-field theory as described above holds without further changes as demonstrated in the Supplemental Material [35].

Our studies also show an asymmetric behavior in β with alignment decreasing faster for pushers ($\beta < 0$) than pullers $\beta > 0$. Again, this agrees with previous studies [17,19] which explained this asymmetry by the observation that head-to-head orientations (which would contribute to $\mathcal{P}_\infty = 0$) are stabilized for pushers due to a stagnation point in front of the swimmer in the swimming frame. Further details on simulations with nonvanishing β can be found in the Supplemental Material [35].

Conclusions.—We investigated the pump formation of active Brownian particles in a harmonic trap with hydrodynamic interactions included. This is an example of a nonequilibrium system whose properties are in striking analogy to a well-known equilibrium system. Specifically, we showed that the self-induced alignment of particles mediated by the flow field they create is in formal agreement with spontaneous magnetization in ferromagnetic materials treated on the mean-field level. Here, particle orientations follow a Boltzmann distribution in an aligning mean flow field which is created by the active particles.

A critical Péclet number, where pump formation sets in, can be determined in analogy to the (inverse) critical temperature of ferromagnets. The mean flow field corresponds to a single regularized Stokeslet. Its strength scales linearly with the particle swimming speed and the regularization parameter ϵ gives the pump radius.

Understanding the nonequilibrium of active particles is one of the challenging questions in statistical physics today. This Letter presents an intriguing example of a nonequilibrium system of active particles which can be mapped onto a classical equilibrium system. With recent advances in colloid physics it would be very interesting to experimentally realize the fluid pump formed by self-induced polar order and validate our predictions.

We thank Andreas Zöttl for helpful discussions and gratefully acknowledge financial support from the Deutsche Forschungsgemeinschaft through the research training group GRK1558.

[1] M. E. Cates, Rep. Prog. Phys. **75**, 042601 (2012).
[2] P. Romanczuk, M. Bär, W. Ebeling, B. Lindner, and L. Schimansky-Geier, Eur. Phys. J. Spec. Top. **202**, 1 (2012).
[3] J. Dunkel, S. Heidenreich, K. Drescher, H. H. Wensink, M. Bär, and R. E. Goldstein, Phys. Rev. Lett. **110**, 228102 (2013).
[4] I. Theurkauff, C. Cottin-Bizonne, J. Palacci, C. Ybert, and L. Bocquet, Phys. Rev. Lett. **108**, 268303 (2012).
[5] J. Palacci, S. Sacanna, A. P. Steinberg, D. J. Pine, and P. M. Chaikin, Science **339**, 936 (2013).
[6] J. Tailleur and M. E. Cates, Phys. Rev. Lett. **100**, 218103 (2008).
[7] Y. Fily and M. C. Marchetti, Phys. Rev. Lett. **108**, 235702 (2012).
[8] G. S. Redner, M. F. Hagan, and A. Baskaran, Phys. Rev. Lett. **110**, 055701 (2013).
[9] I. Buttinoni, J. Bialké, F. Kümmel, H. Löwen, C. Bechinger, and T. Speck, Phys. Rev. Lett. **110**, 238301 (2013).
[10] J. Stenhammar, A. Tiribocchi, R. J. Allen, D. Marenduzzo, and M. E. Cates, Phys. Rev. Lett. **111**, 145702 (2013).
[11] T. J. Pedley and J. O. Kessler, Annu. Rev. Fluid Mech. **24**, 313 (1992).
[12] A. Ordemann, G. Balazsi, and F. Moss, Physica (Amsterdam) **325A**, 260 (2003).
[13] R. A. Simha and S. Ramaswamy, Phys. Rev. Lett. **89**, 058101 (2002).
[14] T. Ishikawa and T. J. Pedley, Phys. Rev. Lett. **100**, 088103 (2008).
[15] D. Saintillan and M. J. Shelley, Phys. Rev. Lett. **100**, 178103 (2008).
[16] A. Baskaran and M. C. Marchetti, Proc. Natl. Acad. Sci. U.S.A. **106**, 15567 (2009).
[17] A. A. Evans, T. Ishikawa, T. Yamaguchi, and E. Lauga, Phys. Fluids **23**, 111702 (2011).
[18] J. J. Molina, Y. Nakayama, and R. Yamamoto, Soft Matter **9**, 4923 (2013).
[19] F. Alarcón and I. Pagonabarraga, J. Mol. Liq. **185**, 56 (2013).
[20] A. Zöttl and H. Stark, Phys. Rev. Lett. **112**, 118101 (2014).
[21] C. Torney and Z. Neufeld, Phys. Rev. Lett. **99**, 078101 (2007).
[22] N. Khurana, J. Blawzdziewicz, and N. T. Ouellette, Phys. Rev. Lett. **106**, 198104 (2011).
[23] A. Zöttl and H. Stark, Phys. Rev. Lett. **108**, 218104 (2012).
[24] J. Tailleur and M. E. Cates, Europhys. Lett. **86**, 60002 (2009).
[25] M. Enculescu and H. Stark, Phys. Rev. Lett. **107**, 058301 (2011).
[26] K. Wolff, A. M. Hahn, and H. Stark, Eur. Phys. J. E **36** (2013).
[27] S. Chattopadhyay, R. Moldovan, C. Yeung, and X. L. Wu, Proc. Natl. Acad. Sci. U.S.A. **103**, 13712 (2006).
[28] C. Lutz, M. Reichert, H. Stark, and C. Bechinger, Europhys. Lett. **74**, 719 (2006).
[29] B. Lincoln, S. Schinkinger, K. Travis, F. Wottawah, S. Ebert, F. Sauer, and J. Guck, Biomed. Microdevices **9**, 703 (2007).
[30] F. Schweitzer, W. Ebeling, and B. Tilch, Phys. Rev. Lett. **80**, 5044 (1998).
[31] M. Rex and H. Löwen, Phys. Rev. Lett. **101**, 148302 (2008).
[32] R. W. Nash, R. Adhikari, J. Tailleur, and M. E. Cates, Phys. Rev. Lett. **104**, 258101 (2010).
[33] A. Pototsky and H. Stark, Europhys. Lett. **98**, 50004 (2012).
[34] J. Vollmer, A. G. Vegh, C. Lange, and B. Eckhardt, Phys. Rev. E **73**, 061924 (2006).
[35] See Supplemental Material at http://link.aps.org/supplemental/10.1103/PhysRevLett.112.238104 for details on the simulation method, formation of the pump state, the mean-field theory, and the effect of swimmer stresslets on pump formation.
[36] D. L. Ermak and J. A. McCammon, J. Chem. Phys. **69**, 1352 (1978).
[37] For thermal diffusion of spherical particles, the rotational (D_R) and translational (D) diffusion coefficients are connected by $D_R = k_B T/(8\pi\eta a^3) = 3D/(4a^2)$.
[38] R. Cortez, L. Fauci, and A. Medovikov, Phys. Fluids **17**, 031504 (2005).
[39] N. W. Ashcroft and N. D. Mermin, *Solid State Physics* (Harcourt, Orlando, 1976).
[40] T. Ishikawa, M. P. Simmonds, and T. J. Pedley, J. Fluid Mech. **568**, 119 (2006).